Applied Catalysis B: Environmental 166–167 (2015) 84–90

Contents lists available at ScienceDirect

Applied Catalysis B: Environmental

journal homepage: www.elsevier.com/locate/apcatb

The effectiveness of indoor photocatalytic paints on NO_x and HONO levels

Adrien Gandolfo[a,1], Vincent Bartolomei[a,1], Elena Gomez Alvarez[a], Sabrine Tlili[a], Sasho Gligorovski[a,*], Jörg Kleffmann[b], Henri Wortham[a]

[a] Aix-Marseille Université, CNRS, Laboratoire Chimie Environnement, FRE 3416, (Case 29), 3 place Victor Hugo, F - 13331 Marseille Cedex 3, France
[b] Physikalische und Theoretische Chemie/FB C, Bergische Universität Wuppertal, Gaußstr. 20, 42119 Wuppertal, Germany

ARTICLE INFO

Article history:
Received 11 September 2014
Received in revised form 27 October 2014
Accepted 8 November 2014
Available online 15 November 2014

Keywords:
Indoor air
Flow reactor
Heterogeneous reactions
Nitrogen oxides
Nitrous acid

ABSTRACT

There is an increasing concern about the indoor air environment, where we spend most of our time. Common methods of improving indoor air quality include controlling pollution sources, increasing ventilation rates or using air purifiers. Photocatalytic remediation technology was suggested as a new possibility to eliminate indoor air pollutants instead of just diluting or disposing them. Titanium dioxide (TiO_2) is a widely used photocatalyst, which is aimed to eliminate organic and inorganic pollutants.

Here, we demonstrate that indoor photocatalytic paints which contain TiO_2 can substantially reduce the concentrations of nitrogen dioxide (NO_2). We show that the efficiency of nitrogen dioxide (NO_2) removal increases with the quantity of TiO_2 in the range 0–7%. The geometric uptake coefficients increase from 5×10^{-6} to 1.6×10^{-5} under light irradiation of the paints. On the other hand, during the reactions of NO_2 with this paint (7% of TiO_2) nitric oxide (NO) and nitrous acid (HONO) are formed. Nitrous acid (HONO) is an important harmful indoor pollutant and its photolysis leads to the formation of highly reactive OH radicals. Maximum conversion efficiencies of NO_2 to HONO and NO of 15% and 33% were observed at 30% RH, respectively.

A dynamic mass balance model applied to typical indoor environment predicts a steady state mixing ratio of 5.6 ppb of HONO released upon light-induced surface reaction of NO_2 with a photocatalytic paint (7% of TiO_2) and considering the photolysis process as the most important loss of HONO.

The quantity of TiO_2 embedded in the paint is of crucial importance with respect to nitrogen oxides NO_2 remediation, but may also influence the formation of harmful intermediates like nitrous acid (HONO), which should be considered for future optimization of photocatalytic paints aimed for indoor applications.

1. Introduction

The influence of indoor air quality on human health is increasingly considered, since people spend the majority of their life indoors. During the last 20 years the design and construction of buildings was radically modified to improve the building energy efficiency and to lower running costs. On the other hand, the new building advances have resulted in more airtight modern home environments, offices, schools and hospitals among others. Thus, the levels of airborne indoor pollutants can reach much higher values compared to outdoor environments [1]. Regarding the gas-phase pollutant NO_2, indoor mixing ratios in the range between 15 and 200 ppb were reported [2–4]. In some indoor environments such as industrial workplaces and homes equipped with gas stoves, peak NO_2 mixing ratios may reach at 1–2 ppm with a 24-h average NO_2 mixing ratio of up to 500 ppb [5].

Weschler and Shields [6] stated that heterogeneous chemistry may play an important role in the indoor environment because the surface to volume ratios (S/V) (m^{-1}) are much higher within indoor settings [4,7] increasing the importance of NO_2 surface reactions. There are several studies reporting "dark" HONO formation during the heterogeneous reactions between gas-phase NO_2 and water layers adsorbed on indoor surfaces [8]. Two recent studies [9,10] have shown that HONO can be formed upon heterogeneous reactions of NO_2 with indoor surfaces in presence of UV light ($300\,nm < \lambda < 400\,nm$).

* Corresponding author. Tel.: +33 413551052; fax: +33 413551060..
E-mail address: saso.gligorovski@univ-amu.fr (S. Gligorovski).
[1] The first two authors contribute equally.

http://dx.doi.org/10.1016/j.apcatb.2014.11.011
0926-3373/

To improve the indoor air quality, photocatalytic materials have been suggested as a new remediation technology, for which titanium dioxide (TiO_2) nanoparticles are either deposited at the surface of the material (such as glass, pavement . . .) or embedded in paints or concrete.

These photo-catalysts, typically activated by UV light (<390 nm) are able to oxidize adsorbed pollutants forming less harmful products, like e.g. CO_2 or adsorbed nitrate. Despite the apparent promise of these materials, extensive trials by authorities across the developed countries have produced relatively little solid evidence in support of their effectiveness for efficient indoor air remediation. Nevertheless, the interest in their extensive application continues to grow [11].

Indeed, several studies claimed the efficiency of TiO_2 nanoparticles to remove the atmospheric pollutants such as nitrogen oxides ($NO_x = NO + NO_2$) and volatile organic compounds (VOCs) [12–18]. Although some promising results have been obtained in the past, also the formation of harmful intermediates has been observed, like for example aldehydes on photocatalytic indoor paints from the decomposition of the organic binder or from reaction of VOCs [17,19] which can certainly affect the durability of the paint. In addition, Langridge et al. [20] have shown that the uptake of NO_2 *on self-cleaning window glass containing* TiO_2 does not represent a permanent sink for gas-phase NO_2, but rather provides a strong daytime source of harmful nitrous acid (HONO). In contrast, Laufs et al. [21] observed a degradation of nitrous acid (HONO) induced by commercial photocatalytic paints aimed for outdoor building facades. Especially, the potential formation of HONO raises important questions regarding the use of photocatalytic materials, because HONO is readily photolyzed leading to OH radical formation [22], which in turn can induce a series of chemical reactions and further aggravate the indoor air quality through formation of secondary pollutants such as ozone and VOCs oxidation products [23]. In addition, HONO is also directly harmful, since its reaction with the amino groups of the nucleotides forms cross-links between the double helix of the DNA leading to mutagenic properties [24–27]. Also, the gas-phase reactions of HONO with amines lead to the formation of nitrosamines in the air [28,29], which are known to exhibit mutagenic and carcinogenic properties [30]. Finally, Sleiman et al. [31] have shown that surface reactions of adsorbed nicotine with gaseous HONO also leads to the formation of nitrosamines. It is noteworthy to mention that HONO was identified and detected for the first time within indoor environments by James N. Pitts, Jr., a prominent scientist in the field of atmospheric chemistry [32,33].

Recently, a new generation of photocatalytic indoor paints containing TiO_2 nanoparticles, has been launched on the market. As these new paints have not yet been rigorously tested, in the present study, optimum conditions with respect to NO_x remediation and HONO formation on photocatalytic paints were studied. For this purpose, in collaboration with the industrial partner ALLIOS we tested new photocatalytic paints with different quantities of TiO_2 nanoparticles aimed for indoor application which are sensitive to UV light in the region between 300 and 400 nm.

2. Materials and methods

2.1. Preparation of photocatalytic paints

The photocatalytic paints were produced by the manufacturer ALLIOS. The type of the photocatalyst used is TITANE P2 in anatase form with a TiO_2 nanoparticles content of ~85%.

TITANE P2 represents a very high purity ultrafine TiO_2 powder with specific surface of 350 m^2/g. In all paints photocatalytically inactive TiO_2 particles in micrometric size are present at the same quantity of 13.4% (w/w). A mixture of grinded additives, called slurry, was prepared with a mass fraction of 35% (w/w) active TiO_2 nanoparticles.

Then, 10, 15 and 20% of this slurry was mixed with the other paint constituents (micrometric TiO_2, and architectural constituent of the paint, i.e. calcium carbonate, $CaCO_3$) to reach 3.5, 5.25 and 7% of photocatalytic active TiO_2 nanoparticles (w/w), respectively. Note that, the photocatalyst in the paint is sensitive to the UV light. The replacement of $CaCO_3$ with the slurry induces a change in the density which in turn has an impact on the paint stability. Therefore, the maximum allowed mass fraction of TiO_2 nanoparticles in the paint is 7%. Note, that the slurry is absent in the paint without TiO_2 nanoparticles.

The prepared paint was then applied *on one side of* glass plates with dimensions 29 cm × 1.9 cm (length × width) by a well-established *drying* procedure developed by the manufacturer. This procedure allows homogeneous, uniform and reproducible wet film with 100 μm thickness. The glass plates were stored during 21 days in an oven ventilated by clean air at 23 °C and 55% relative humidity. The prepared glass plates were then delivered to our laboratory in order to assess the impact of the photocatalytic paints on NO_x and HONO levels. The latter was achieved by studying the NO_2 heterogeneous reactivity in a flow tube photo-reactor.

2.2. Flow tube photo-reactor

The experimental set-up was previously described in detail [9,10]; hence, here only a brief description is given.

The kinetic experiments were performed in a double-wall flow tube photo-reactor connected to a thermostatic bath which allowed operation at different temperatures. The dimensions of the flow reactor were chosen to ensure conditions for gas-phase laminar flow. The flow tube is a cylinder of 131 cm^3 made of borosilicate glass. The glass plate was inserted into the flow tube reactor with the painted side upward oriented. The length of the glass plate is almost identical with the dimension of the flow reactor which allows to be perfectly fitted into the reactor without perturbation of the laminar flow. Inside the flow tube, a movable injector is inserted which allows to vary the exposed length of the paint. The flow tube and six lamps (Philips TL-D 18 W, 340–400 nm, λ_{max} = 368 nm, length = 60 cm) that could be operated individually were placed in a stainless steel box. Because the paints were applied only on one side of the glass plate, the lamps were placed in the following manner: four lamps were mounted on the box above the reactor and two were placed in the upper left and right corner of the box. The spectral irradiance of these lamps was already characterized in our previous study [10] and compared to the solar light intensity which could penetrate indoors which allows to perform the experiments under relevant indoor conditions.

A certified mixture of NO_2 (100 ppm) in Helium (Praxair) was connected to a mixing loop fed by synthetic air (Linde gas 5.0, flow controller, Brooks SLA, 0–500 ml/min) to allow a first dilution before the introduction of the NO_2 through the movable injector (flow controller, Brooks SLA, 0–20 ml/min). In order to simulate realistic indoor conditions all the experiments were performed at 40 ppb of NO_2. A sheath flow of 980 ml/min (Linde gas 5.0, flow controller Brooks SLA 0–1 l/min) was fed to a humidification system before its introduction in the reactor. Humidity was adjusted by splitting this sheath flow in two fluxes controlled by needle valves, one of dry air flow and the other humidified by bubbling through deionised water. A mixing of these two flows at different ratios generated a carrier gas at controlled relative humidity. Downstream of this device, a hygrometer "Hygrolog NT2" (Rotronic) with a

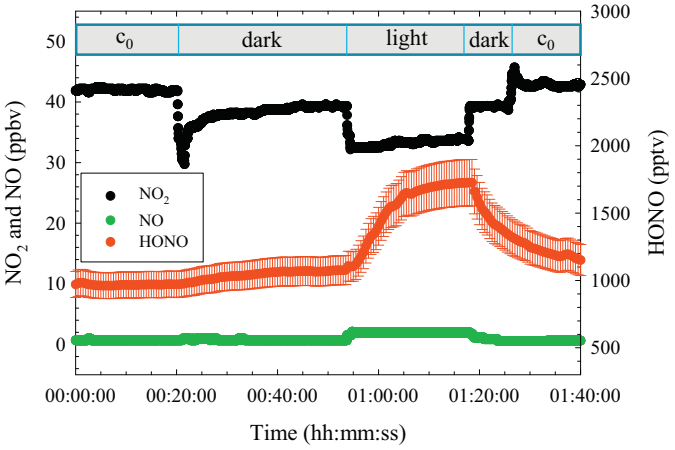

Fig. 1. Typical experiment of NO_2 uptake (dark line) and build-up of NO (green line) and HONO (red line) in the dark and under light irradiation of the photocatalytic paint with 7% of TiO_2 nanoparticles at 40 ppb initial mixing ratio of NO_2. (For interpretation of the references to color in this figure legend, the reader is referred to the web version of the article.)

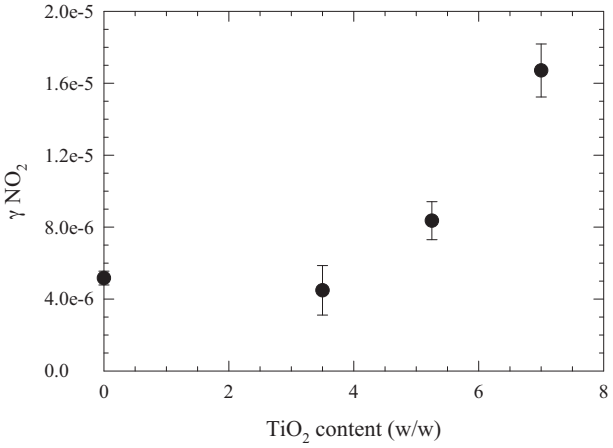

Fig. 2. NO_2 uptake coefficient as a function of the TiO_2 nanoparticles content at NO_2 mixing ratio of 40 ppb, 20 W m^{-2} UVA and RH of 40%. The error bars are derived from the uncertainties associated to the estimation of the uptake coefficients.

"HygroClip SC04" probe measured the resulting humidity on-line (±1.5% RH accuracy).

At the reactor exit, the effluent of the reactor was diluted with a flow of air of 1.2 l/min which is controlled by critical flow restricting orifice at constant pressure. A manometer was placed to allow constant air delivery during all the experiment. Then, the flow rate of the diluted effluent was sufficient to feed both, the NO_x and HONO analysers, giving a total flow of 2.2 l/min.

NO_x, NO_2 and NO concentrations were simultaneously measured by a chemiluminescence instrument (Eco Physics, model CLD 88p) associated with a photolytic (metal halide lamp) converter (Eco Physics, model PLC 860). This instrument is very sensitive with a detection limit of 50 ppt and requires a minimum gas flow rate of 730 ml/min.

The gas phase HONO concentration was measured using a LOng Path Absorption Photometer (LOPAP, QUMA). The instrument has a detection limit of 2–3 ppt and a total accuracy of ±10% with an actual time response of about 5 min under the operation conditions applied (gas flow 1 l/min). A detailed description of its operation principle and procedure can be found in the literature [34–36].

NO_2 photodissociates in the wavelength region (340–420 nm) emitted by the lamps. Control experiments were performed to confirm the chemical inactivity of the flow tube wall surfaces and to evaluate the contribution of NO_2 photolysis. For this purpose an empty flow tube was flushed with gas-phase NO_2 and exposed to the UV light. For the residence time of 7.5 s under our experimental conditions the photolysis of NO_2 was 7%, which was considered for the data evaluation of the NO_2 experiments with the paints.

3. Results and discussion

Uptake of NO_2 on photocatalytic paints containing 0, 3.5, 5.25 and 7% of TiO_2 nanoparticles was studied in the horizontal flow tube reactor.

Fig. 1 shows typical profiles of NO_2, NO and HONO under dark conditions and in presence of light.

The effect of the quantity of TiO_2 nanoparticles on the uptake coefficients of NO_2 (γ_{NO_2}) is shown in Fig. 2. For details on the calculation of γ, see SI.

As expected, γ_{NO_2} increased with the quantity of introduced TiO_2 nanoparticles in the paints, which *a priori* would indicate that the higher the content of TiO_2 nanoparticles, the more efficiently photocatalytic paints work as a remediation material. However, the paint containing 3.5% of TiO_2 nanoparticles exhibits almost the same uptake coefficient as the one with 0% of TiO_2 nanoparticles. The reason for this observation could be the scavenging of OH radicals formed by the reaction of water with the valence band hole (see below (R-4)) [21], e.g. by any organic binder and/or additives in the paint. Thus, at low TiO_2 nanoparticles content OH may not be available for oxidation of adsorbed NO_2. Only with increasing TiO_2 content the formed radicals exceed these losses and they are available for reaction with NO_2.

The uptake coefficient for the paint without photocatalytic TiO_2 was found to be 5×10^{-6} and increased up to 1.6×10^{-5} for the photocatalytic paint with 7% of TiO_2 nanoparticles. However, whilst the photocatalytic paint with 7% of TiO_2 efficiently eliminates gas-phase NO_2, it gives rise to the gaseous reaction products NO and HONO as shown in Fig. 3.

The NO yield is strongly increasing with the TiO_2 nanoparticle content. On the other hand, gas-phase HONO is formed only with the paint containing 7% of TiO_2 nanoparticles. Both species are formed through a reaction mechanism which has been postulated in the literature [37,38]. Briefly, the photolysis of TiO_2 ($\lambda < 390$ nm)

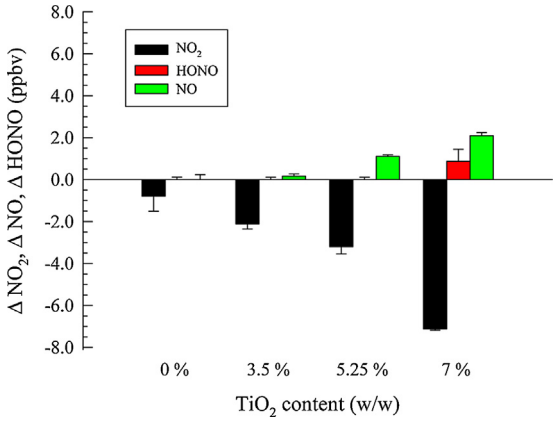

Fig. 3. NO_2 loss, NO and HONO formation on photocatalytic paints with 0, 3.5, 5.25 and 7% of TiO_2 nanoparticles at NO_2 mixing ratio of 40 ppb and RH of 40%. Error bars indicate the standard deviation from four independent measurements.

leads to the formation of an electron in the conduction-band (e^-_{cb}) and a valence-band hole (h^+_{vb}) (R-1).

$$TiO_2 + h\nu \rightarrow e^-_{cb} + h^+_{vb} \quad \text{(R-1)}$$

The reaction mechanism of HONO formation by photocatalytic reactions on TiO_2 surface was postulated by Ndour et al. [38] as follows:

$$e^-_{cb} + O_2 \rightarrow O_2{}^- \quad \text{(R-2)}$$

$$NO_2 + O_2{}^-(+H^+) \rightarrow NO_2{}^-(HONO) + O_2 \quad \text{(R-3)}$$

$$h^+_{vb} + H_2O \rightarrow OH + H^+ \quad \text{(R-4)}$$

$$NO_2 + OH \rightarrow HNO_3 \quad \text{(R-5)}$$

leading to the catalytic net reaction:

$$2NO_2 + H_2O \xrightarrow{+h\nu,TiO_2} HONO + HNO_3 \quad \text{(R-6)}$$

Thus, the disproportionation reaction of NO_2, which has been also suggested as a night-time source of HONO in the atmosphere [8], can be photocatalytically enhanced in the presence of TiO_2 [20].

We performed blank experiments irradiating the glass reactor without the paint sample and obtained that a minor fraction of only 7% of NO_2 was photolysed. The obtained results with respect to the uptakes of NO_2 and NO and HONO formed were then corrected subtracting NO and HONO formation from these blank experiments. However, besides gas phase photolysis of NO_2 the NO may also be formed from adsorbed NO_2 on the highly porous paint surface which is absent in the blank experiments in the empty reactor.

$$NO_2(ads) \xrightarrow{+h\nu,TiO_2} NO(ads) + O(^3P) \quad \text{(R-7)}$$

In this case, the reaction between adsorbed NO and surface OH radicals (R-4) may be an additional source of gaseous HONO.

$$NO(ads) + OH(ads) \xrightarrow{TiO_2} HONO \quad \text{(R-8)}$$

Indications for the plausibility of reaction (R-8) are (a) the linear increase of the NO quantity and (b) the non-linear dependence of HONO on the TiO_2 nanoparticle content in Fig. 3. Assuming that both, the amount of adsorbed NO_2 (and subsequent NO) and the yield of OH radicals increase linearly with the TiO_2 nanoparticle content, both observations can be explained by reaction (R-8). Alternatively, reactions (R-3) or (R-9) may also explain the observed HONO formation.

$$NO_2 + e^- + H^+ \rightarrow HONO \quad \text{(R-9)}$$

However, in this case the HONO yield is expected to linearly increase with the TiO_2 content which was not observed, pointing to (R-8) as a more plausible HONO source reaction. For the future, additional measurements are proposed to distinguish between the different HONO source reactions.

The effect of light intensity on the uptake coefficients of NO_2 on different photocatalytic paints is shown in Fig. 4.

Clearly, the uptake kinetics of NO_2 on the photocatalytic paints is increasing with light intensity, which is most pronounced for the paint with the maximum content of TiO_2 nanoparticles, i.e. 7%. For that paint the photoenhanced uptake coefficient is almost linearly dependent on the irradiance. The uptake coefficients of NO_2 increase by a factor of four from 4×10^{-6} in the dark up to 1.6×10^{-5} in presence of 20 W m^{-2} irradiance. For the paint with 0% and 3.5% of TiO_2 nanoparticles there is no significant dependence of γ_{NO_2} with the light intensity, which is in line with the TiO_2 dependence of γ_{NO_2}, see Fig. 2, explained by the scavenging of the photocatalytically formed OH radicals. For paint containing 5.25% of TiO_2 nanoparticles the uptake coefficients exhibit untypical non-linear increase with the light intensity. This observation may be explained

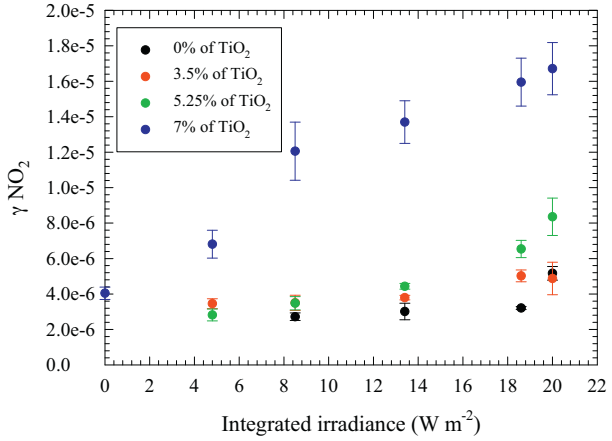

Fig. 4. Uptake coefficients as a function of the integrated irradiance (340 nm < λ < 400 nm) at NO_2 mixing ratio of 40 ppb, on photocatalytic paints with 0–7% of TiO_2 and RH of 40%. Error bars are derived from the uncertainties associated with the calculation of γ_{NO_2}.

by a threshold limit of scavenged OH radicals by the paints, which is only exceeded at very high UVA irradiance.

The yields of conversions of the two products NO and HONO formed during the heterogeneous reactions of NO_2 with the photocatalytic paints as a function of the spectral irradiance, are presented in Fig. 5. The conversion yields of NO and HONO were calculated as a ratio of $\Delta NO/\Delta NO_2$ and $\Delta HONO/\Delta NO_2$, respectively.

In contrast to photocatalytic outdoor paints [21] here we observe significant NO_2 to NO conversion yield which increases with the light intensity indicating a photocatalytic formation on the paint containing 7% of TiO_2 nanoparticles. The harmful pollutant HONO is also formed with lower yields (ca. 4%) which are almost independent on the light intensity up to ca. 18 W m^{-2}. This result showing the formation of HONO in function of light intensity is an important outcome considering that the light intensity is attenuated in the indoor environments [39] and highly variable depending on the location of the building, the season of the year, orientation of the room and the size and nature of the windows [40]. Concerning the paints with 0, 3.5 and 5.25% of TiO_2, a very small quantity of NO and HONO was formed only at 20 W m^{-2} irradiance.

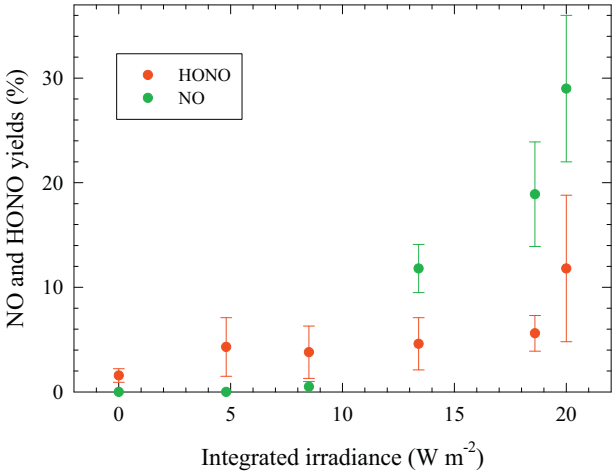

Fig. 5. HONO and NO yields from conversion of NO_2 (40 ppb) on a photocatalytic paint with 7% of TiO_2 nanoparticles as a function of the integrated irradiance (340 nm < λ < 400 nm) at 40% RH. Error bars indicate the standard deviation from four independent measurements.

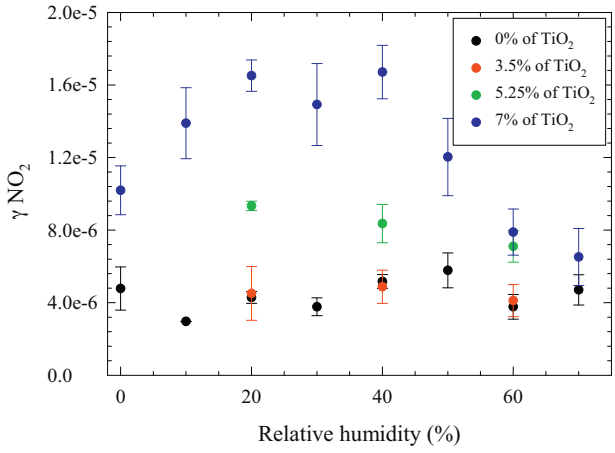

Fig. 6. NO_2 uptake coefficients on photocatalytic paints with 0–7% of TiO_2 nanoparticles as a function of relative humidity obtained at 40 ppb of NO_2 in presence of 20 W m^{-2} UVA.

Indoor humidity is another important parameter controlled by ventilation and outdoor climatic conditions. Ventilation must be adequate to remove and dilute pollutants and humidity generated indoors. Relative humidity (RH) varies over a broad range in different indoor environments [1]. Changes of RH imply a change in the amount of adsorbed water on the indoor surfaces and the occurrence of adsorbed surface films. Here, the NO_2 uptake coefficients concerning the paints without TiO_2 and with 3.5% of TiO_2 nanoparticles are almost independent of the RH, whereas the NO_2 uptake only slightly decreases with humidity on the paint containing 5.25% of TiO_2 nanoparticles (Fig. 6).

On the other hand, for the paint containing 7% of TiO_2 nanoparticles a maximum in the reactivity is observed at ca. 30% RH. Uptake coefficients increase from 1×10^{-5} at 0% RH, reach a maximum of $\sim 1.6 \times 10^{-5}$ at 20–40% RH and decrease to 6×10^{-6} at 70% RH. It seems that water first promotes the uptakes of NO_2 on the paint containing 7% of TiO_2 nanoparticles. However, the decrease of the uptake coefficient observed at higher humidity indicates that water also blocks adsorption sites and thus inhibits the access of NO_2 to the surface.

A similar humidity dependence of the NO_2 uptake on an outdoor photocatalytic paint was observed by Laufs et al. [21]; the only difference is that, in the present study, the maximum is shifted to higher RH. Thus, in good agreement to the study of Laufs et al. [21] photocatalytic oxidation of NO_2 is proposed by reactions (R-4) and (R-5). Here, adsorbed water is necessary to generate OH radicals, which further oxidize NO_2. In contrast, adsorbed water blocks active photocatalytic sites reducing again the reactivity at high humidity.

It is interesting to note that the observed maximum of the uptake of NO_2 at ~30% RH corresponds closely to realistic indoor conditions. According to ASHRAE Standard 55 [41], indoor humidity levels should be maintained between 30% and 65% for optimum comfort.

The yields of formation of gaseous NO and HONO at different relative humidities are summarized in Table 1. At 30% RH, about 50% of the NO_2 loss under light irradiation of the photocatalytic paint (7% TiO_2) gives rise to production of the gas phase products HONO and NO. The HONO yield was 4% at 10% RH, and increased up to 15% at 30% RH (Table 1). The yield of NO was about 7% at 10% RH and reached 33% at 40% RH.

Whilst the HONO and NO yields were increasing with increasing humidity it is interesting to note that at 50 and 60% RH there was no measurable production of NO and HONO from the still significant uptake of NO_2, the reason for which is still unclear.

The sum of both NO and HONO yields was lower than 50% for the range of RH between 10 and 40% which in turn suggests that the reaction between gas-phase NO_2 and the photocatalytic paints may produce non-volatile products such as adsorbed nitric acid/nitrate (HNO_3/NO_3^-) in line with the proposed net reaction (R-6). Indeed, the formation of adsorbed HNO_3/NO_3^- on photocatalytic paints aimed for outdoor facades was previously confirmed [21].

3.1. Implications for typical indoor environments

Applying a dynamic mass balance model, we estimate the implications of a photocatalytic paint containing 7% of TiO_2 assuming an average sized indoor room that is 2.5 m high, 5 m wide and 4 m long, hence with a total volume of 50 m^3. Also, it is assumed that one side of the room represents a large window with the surface of 10 m^2 and the other sides of the room are wall with the surfaces of 10 m^2 and 12.5 m^2, respectively. In order to simulate more realistic conditions we minimize the area of the walls which are exposed to the direct sunlight. For this reason, we assume that only one half of one of the side walls ($S = 6$ m^2) is irradiated with direct sunlight of 9 W m^{-2} [9,10] for the wavelength region $300 < \lambda < 400$ nm yielding a HONO emission rate of 0.8 mg h^{-1} upon light induced heterogeneous reactions of 40 ppb of NO_2 with the painted wall at 30% RH.

Considering an average air-exchange rate of 0.56 h^{-1} [42], we can estimate the concentration of HONO produced by the photocatalytic paint (7% of TiO_2).

Assuming a constant HONO production rate under direct light irradiation the concentrations of HONO can be represented as:

$$c_a(t) = \frac{E_R}{k_{AER}V + J(\mathrm{HONO})V_1} + \left(c_0 - \frac{E_R}{k_{AER}V + J(\mathrm{HONO})V_1}\right) \times e^{-(k_{AER}+J(\mathrm{HONO}))t} \quad (1)$$

where $c_0 = 0$, is the initial HONO concentration in mg m^{-3}, t is the time (h), $c_a(t)$ is the gaseous concentration of HONO (mg m^{-3}), k_{AER} is the air exchange rate constant (h^{-1}), E_R is the mass emission rate of HONO induced by the photocatalytic paint (mg h^{-1}), V_1 represents the volume of the room that is irradiated with the direct sunlight ($300 < \lambda < 400$ nm) and V is the total volume of the room (50 m^3).

We have shown that HONO is dissociated under direct light irradiation which penetrates indoors and represents the main source of OH radicals [22]. Therefore, we assume that the most important HONO sink is the photolysis. The photolysis frequency of HONO was estimated assuming direct light irradiation of 9 W m^{-2} as $J(\mathrm{HONO}) = 7.2 \times 10^{-4}$ s^{-1}.

Assuming that only one third of the volume of the room is directly irradiated with 9 W m^{-2} during certain period of the day we obtain the HONO levels in function of time produced by the photocatalytic paint which contains 7% of TiO_2 at 30% RH and 40 ppb of NO_2 (Fig. 7).

Table 1
HONO and NO yields derived from the heterogeneous reaction of NO_2 (40 ppb) with the photocatalytic paint containing 7% of TiO_2 nanoparticles under UVA irradiation (20 W m^{-2}). Error bars represent 1σ precision.

RH/%	HONO yield/%	NO yield/%
0	No production	No production
10	4 ± 1	7 ± 7
20	13 ± 3	31 ± 4
30	15 ± 4	33 ± 4
40	12 ± 6	29 ± 7
50	No production	No production
60	No production	No production

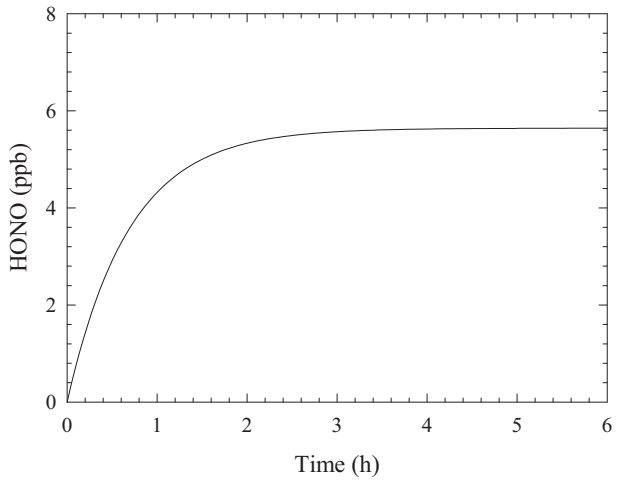

Fig. 7. The estimated mixing ratio of HONO emitted by photocatalytic paint containing 7% of TiO_2 (w/w) at 40 ppb of NO_2 and 30% RH in function of time. Dash line represents the steady state of HONO.

The total HONO mixing ratio increases with the time reaching a steady state of 5.6 ppb after 3 h. This HONO value is 3.5 times higher (under similar assumed conditions) than the HONO (1.6 ppb) released by non-photocatalytic paint, lacquer and glass altogether that we previously reported [9] demonstrating that certain precautions should be taken whilst optimizing the photocatalytic materials aimed for air purification in the indoor settings.

The influence of indoor air quality on human health is increasingly considered, since people spend the majority of their life indoors. With this respect, the emerged results on behalf of HONO formation become of great importance.

4. Conclusion and outlook

Currently, photocatalytic wall paints are not well optimized, and their development with suitable properties for the removal of VOCs and NO_x in realistic indoor settings seems to be a challenging task. This work contributes towards optimization of the photocatalytic paints sensitive to UV light with respect to the introduced quantity of photocatalytic TiO_2 nanoparticles which may regulate the concentrations of harmful pollutants like NO_x and HONO in the indoor environment.

We demonstrated that the quantity of TiO_2 embedded in the paint is crucial for future optimization of photocatalytic paints aimed for indoor applications with respect to the photocatalytic uptake of NO_2 and the formation of HONO and NO. An increase of the quantity of photocatalytic TiO_2 nanoparticles increases the uptake efficiency for NO_2. Unfortunately for the tested paint, this also results in the production of harmful gas-phase by-products such as HONO in indoor air.

Considering that the UV portion of the light is attenuated [39] in the indoor environments, an important outcome of this study is that HONO would be formed on the photocatalytic paints containing 7% of TiO_2 nanoparticles independently on the light intensity in the near-UV region.

A dynamic mass balance model was applied to predict the time evolution of HONO in a real indoor environment. A steady daytime state mixing ratio of HONO has been estimated at 5.6 ppb assuming a contribution from a photocatalytic paint with 7% of TiO_2 (w/w) at 30% RH and 40 ppb of NO_2 and considering the photolysis of HONO as the most important loss process. Further studies of the heterogeneous chemistry on photocatalytic indoor paints [43] with TiO_2 nanoparticles not only focused on NO_x but also on VOCs and its associated secondary constituents (e.g. formation of harmful aldehydes) are recommended in order to optimize the application of these paints in various indoor environments as an alternative remediation technology for purification of indoor air. In addition, future studies should also include application of new catalysts active also in the visible and using typical indoor visible light sources.

Acknowledgements

To the memory of the prominent scientist James N. Pitts Jr. who gave a tremendous contribution in the field of atmospheric chemistry in both outdoor and indoor environments.

This work is a contribution to the LABEX SERENADE (n° ANR-11-LABX-0064) funded by the « Investissements d'Avenir », French Government program of the French National Research Agency (ANR) through the A*Midex project (No. ANR-11-IDEX-0001-02).

Appendix A. Supplementary data

Supplementary data associated with this article can be found, in the online version, at http://dx.doi.org/10.1016/j.apcatb.2014.11.011.

References

[1] C.J. Weschler, Indoor Air 21 (2011) 205–218.
[2] C.J. Weschler, Atmos. Environ. 43 (2009) 153–169.
[3] K. Lee, J. Xue, A.S. Geyh, H. Ozkaynak, B.P. Leaderer, C.J. Weschler, J.D. Spengler, Environ. Health Perspect. 110 (2002) 145–149.
[4] T. Wainman, C.J. Weschler, P.J. Lioy, J. Zhang, Environ. Sci. Technol. 35 (2001) 2200–2206.
[5] C. Monn, Atmos. Environ. 35 (2001) 1–32.
[6] C.J. Weschler, H.C. Shields, Environ. Sci. Technol. 31 (1997) 3719–3722.
[7] C.J. Weschler, Indoor Air 14 (Suppl. 7) (2004) 184–194.
[8] B.J. Finlayson-Pitts, L.M. Wingen, A.L. Sumner, D. Syomin, K.A. Ramazan, Phys. Chem. Chem. Phys. 5 (2003) 223–242.
[9] E. Gómez Alvarez, M. Sörgel, S. Gligorovski, S. Bassil, V. Bartolomei, B. Coulomb, C. Zetzsch, H. Wortham, Atmos. Environ. 95 (2014) 391–399.
[10] V. Bartolomei, M. Sörgel, S. Gligorovski, E.G. Alvarez, A. Gandolfo, R. Strekowski, E. Quivet, A. Held, C. Zetzsch, H. Wortham, Environ. Sci. Pollut. Res. 21 (2014) 9259–9269.
[11] P. Berdhal, H. Akbari, Lawrence Berkeley National Laboratory Report, 2008.
[12] C.H. Ao, S.C. Lee, C.L. Mak, L.Y. Chan, Appl. Catal. B: Environ. 42 (2003) 119–129.
[13] H. Destaillats, M. Sleiman, D.P. Sullivan, C. Jacquiod, J. Sablayrolles, L. Molins, Appl. Catal. B: Environ. 128 (2012) 159–170.
[14] J.S. Dalton, P.A. Janes, N.G. Jones, J.A. Nicholson, K.R. Hallam, G.C. Allen, Environ. Pollut. 120 (2002) 415–422.
[15] S. Devahasdin, C. Fan, K. Li, D.H. Chen, J. Photochem. Photobiol. A: Chem. 156 (2003) 161–170.
[16] T. Maggos, J.G. Bartzis, P. Leva, D. Kotzias, Appl. Phys. A 89 (2007) 81–84.
[17] T. Salthammer, F. Fuhrmann, Environ. Sci. Technol. 41 (2007) 6573–6578.
[18] S. Wang, H.M. Ang, M.O. Tade, Environ. Int. 33 (2007) 694–705.
[19] J. Auvinen, L. Wirtanen, Atmos. Environ. 42 (2008) 4101–4112.
[20] J.M. Langridge, R.J. Gustafsson, P.T. Griffiths, R.A. Cox, R.M. Lambert, R.L. Jones, Atmos. Environ. 43 (2009) 5128–5131.
[21] S. Laufs, G. Burgeth, W. Duttlinger, R. Kurtenbach, M. Maban, C. Thomas, P. Wiesen, J. Kleffmann, Atmos. Environ. 44 (2010) 2341–2349.
[22] E. Gómez Alvarez, D. Amedro, A. Charbel, S. Gligorovski, C. Schoemaecker, C. Fittschen, J.-F. Doussin, H. Wortham, Proc. Natl. Acad. Sci. U.S.A. 110 (2013) 13294–13299.
[23] Y. Sadanaga, J. Matsumoto, Y. Kajii, J. Photochem. Photobiol. C: Photochem. Rev. 4 (2003) 85–104.
[24] E.A. Harwood, P.B. Hopkins, S.T. Sigurdsson, J. Org. Chem. 65 (2000) 2959–2964.
[25] J.J. Kirchner, P.B. Hopkins, J. Am. Chem. Soc. 113 (1991) 4681–4682.
[26] J.J. Kirchner, S.T. Sigurdsson, P.B. Hopkins, J. Am. Chem. Soc. 114 (1992) 4021–4027.
[27] R. Shapiro, S. Dubelman, A.M. Feinberg, P.F. Crain, J.A. McCloskey, J. Am. Chem. Soc. 99 (1977) 302–303.
[28] J.N. Pitts, D. Grosjean, K. Van Cauwenberghe, J.P. Schmid, D.R. Fitz, Environ. Sci. Technol. 12 (1978) 946–953.
[29] J.N. Pitts, Environ. Health Perspect. 47 (1983) 115–140.
[30] D. Shapley, Science 191 (1976) 268–270.
[31] M. Sleiman, L.A. Gundel, J.F. Pankow, P. Jacob, B.C. Singer, H. Destaillats, Proc. Natl. Acad. Sci. U.S.A. 107 (2010) 6576–6581.
[32] J.N. Pitts Jr., T.J. Wallington, H.W. Biermann, A.M. Winer, Atmos. Environ. 19 (1985) 763–767.
[33] J.N. Pitts, H.W. Biermann, E.C. Tuazon, M. Green, W.D. Long, A.M. Winer, J. Air Pollut. Control Assoc. 39 (1989) 1344–1347.

[34] J. Heland, J. Kleffmann, R. Kurtenbach, P. Wiesen, Environ. Sci. Technol. 35 (2001) 3207–3212.
[35] J. Kleffmann, J. Heland, R. Kurtenbach, J. Lorzer, P. Wiesen, Environ. Sci. Pollut. Res. 9 (4) (2002) 48–54.
[36] J. Kleffmann, P. Wiesen, Atmos. Chem. Phys. 8 (2008) 6813–6822.
[37] Y. Ohko, Y. Nakamura, A. Fukuda, S. Matsuzawa, K. Takeuchi, J. Phys. Chem. C 112 (2008) 10502–10508.
[38] M. Ndour, B. D'Anna, C. George, O. Ka, Y. Balkanski, J. Kleffmann, K. Stemmler, M. Ammann, Geophys. Res. Lett. 35 (2008) L05812.
[39] W.W. Nazaroff, G.R. Cass, Environ. Sci. Technol. 20 (1986) 924–934.
[40] S. Gligorovski, C.J. Weschler, Environ. Sci. Technol. 47 (2013) 13905–13906.
[41] Anon., A.S. of Heating, Refrigerating, A.-C. Engineers, Energy Efficient Design of Low Rise Residential Buildings, American Society of Heating, Refrigerating and Air-Conditioning Engineers, 2004.
[42] L.A. Wallace, S.J. Emmerich, C. Howard-Reed, J. Expos. Anal. Environ. Epidemiol. 12 (2002) 296–306.
[43] S. Gligorovski, H. Wortham, J. Kleffmann, New Directions, Atmos. Environ. 99 (2014) 568–570.